examined the use of variable organic solvents in the rinsing step to enhance the efficiency of protein detection in tissue [9] (Table 3.1). They showed mass spectra obtained from mouse brain sections with or without rinsing using chloroform, acetone, or hexane, and found that the predominant signals in the vicinity of $m/z$ 700 are abolished with rinsing procedure, and conversely, the number of peaks derived from proteins at a high molecular weight (i.e., 5000 < $m/z$) increased more than 40% after rinsing. We consider that this treatment also helps remove salts, a detrimental factor that otherwise interferes with the matrix–analyte cocrystallization process and thus degrades sensitivity, particularly for large proteins, while also complicating the spectrum assignment by producing both protonated and cationated molecular ions [10].

Figure 3.6 shows an example of protein imaging in the mouse brain section. With a proper sample preparation

**TABLE 3.1 The Average Number of Detected Compounds from Rat Brain Treated with Various Organic Solvents [9]**

| Treatment | $n$ | Number of Detected Compounds ± Standard Deviation (%) | Increase in Detection (%) |
|---|---|---|---|
| Chloroform | 10 | 81 ± 22 | 34 |
| Hexane | 5 | 75 ± 28 | 25 |
| Toluene | 5 | 68 ± 22 | 13 |
| Xylene | 5 | 86 ± 13 | 44 |
| Acetone | 5 | 64 ± 29 | 7 |
| Untreated | 10 | 60 ± 34 | 0 |

The average number of detected compounds and calculated increase detection for peptides/proteins of $m/z$ > 5000 is determined from the mass spectra recorded on untreated rat brain sections versus organic solvent-treated ones.
$n$, number of experiments.

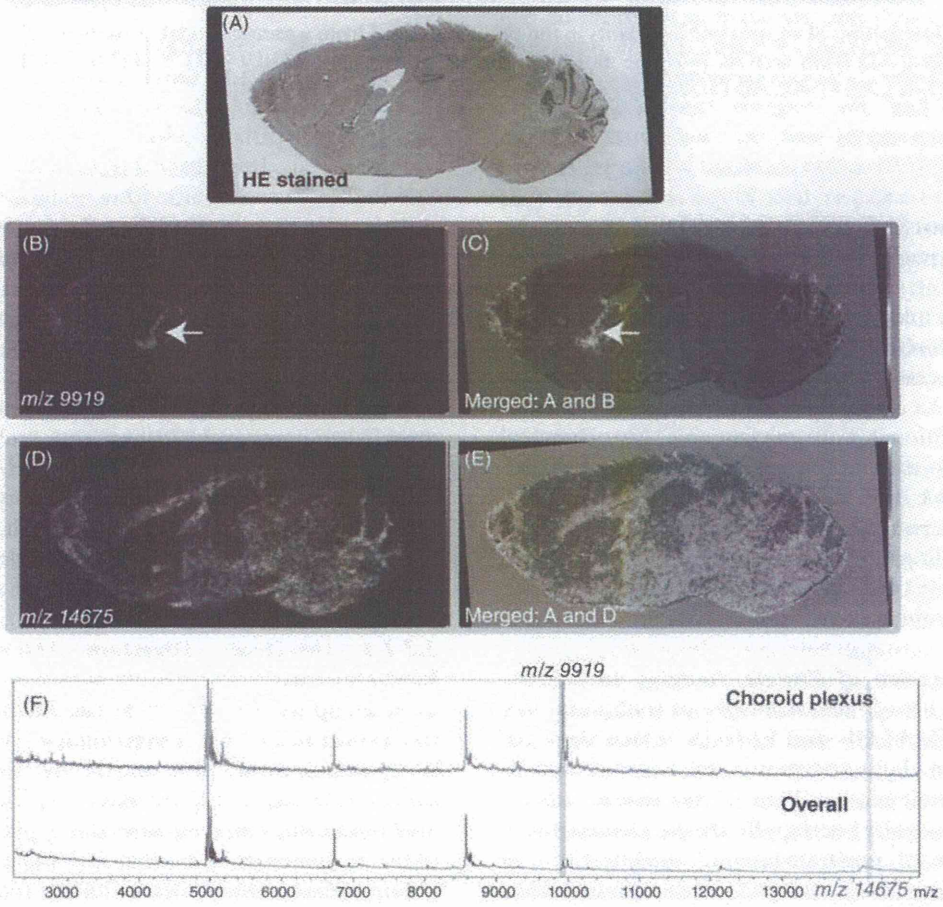


**FIGURE 3.6** With proper sample preparation procedure, IMS facilitates simultaneous imaging of multiple proteins in a single tissue section. The figure shows the ion distribution images for mass peaks at $m/z$ 9919 (B) and 14675 (D), and a microscopic observation of the same mouse brain section stained with HE after IMS measurement (C and E). The ion at $m/z$ 14675 was localized in the white matter region, while $m/z$ 9919 was found in choroid plexus (B and C). Averaged mass spectra from the choroid plexus and entire brain region (overall) were also presented (F).

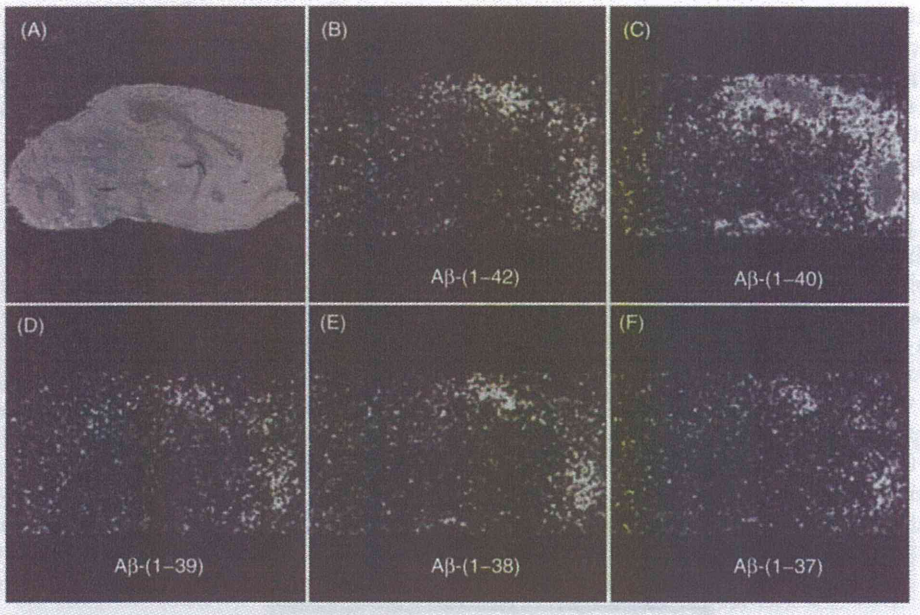


**FIGURE 3.7** Distribution of six amyloid β variants in the tissue prepared from a mouse model of Alzheimer's disease. A. Optical image of the sagittal AD brain section. B–F. The molecular images of *m/z* 4515, 4330.9, 4231.7, 4132.6, and 4075.5 shows the distribution of Aβ-(1-42), Aβ-(1-40), Aβ-(1-39), Aβ-(1-38), and Aβ-(1-37), respectively [14].

procedure shown in Figure 3.5, MALDI-IMS provides simultaneous imaging of multiple proteins in a single tissue section at a time. We additionally note that researchers can histochemically stain the tissue sections which are measured by IMS after removal of the matrix and fixation procedure (in this case, immersed in methanol for 5 min). As can be seen in Figure 3.6, in conjunction with traditional light-microscopic histochemical observation, ion distribution images obtained by IMS provides valuable information regarding molecular distribution; this example demonstrates that ion at *m/z* 9919 is a specific protein expressed by cells of choroid plexus, while *m/z* 14675 is localized in the white matter region of the brain.

***3.2.1.3 Application of Protein Imaging to Disease Model Mice*** One of the advantages of traditional MS, including both MALDI- and ESI-MS, is that they can distinguish even slight structural variations of analyte molecules by their masses. Due to this unique advantage, MS has frequently been applied to the identification/characterization of posttranslational modifications in modern proteome researches [12]. In this context, IMS also enables the distinct detection of the protein molecular species as well as the visualization of the distribution of these species on the tissue sections. As an excellent example, in the Stoeckli et al. study, amyloid β molecular species were visualized, which is generated by cleaving the amyloid precursor protein at a different cleavage site [13]. They revealed the distinct distribution of five amyloid β variants in the brain sections prepared from a mouse model of Alzheimer's disease [3,14] (Figure 3.7).

From the analytical aspect, while traditional and well-established immunohistochemistry technique requires specific antibodies which recognize each protein variant, and generation of such antibodies is a quite time-consuming procedure, on the other hand, IMS could determine the distribution of protein molecular variants at once, even *via* a simple protocol.

***3.2.1.4 On-Tissue Digestion Method*** Traditional MALDI is used to generate intact molecular ions of proteins up to *m/z* 100,000. In the current IMS technology, however, the upper mass limit of protein detection is approximately 40 kDa because the detection sensitivity severely falls at higher mass [15]. This is a considerable limitation which narrows the application capability of this technology. As another important problem, insoluble proteins to the matrix solution, such as membrane proteins, which is a protein molecule that is attached to the membranes, are difficult to be extracted into the applied matrix solutions and thus hardly crystallize with matrix, and they were in turn difficult to detect. On this

regard, on-tissue digestion method in which proteins are denatured and enzymatically digested has been developed as an effective solution for these problems [16–18]. In this method, by cleaving large proteins, such proteins can be measured as digested proteins which are observed mainly in the mass range of $900 < m/z < 3000$. The protein digestion process also makes it easier to perform tandem mass spectrometry (MS/MS), thus to identify the molecular species directly on the tissue section [16,18] (Figure 3.8). For all these reasons, on-tissue digestion is an attractive alternative method for detecting proteins that cannot be ionized by standard methods. We previously studied this method and found that this process was enhanced by a heat-denaturation process (80°C, for 10 h) and the use of a detergent-supplemented trypsin solution (200 mg/mL trypsin in 25 mM $NH4HCO_3$ and 20 mM n-octylglucoside) (Figure 3.9; see detail protocol for Setou et al. [19]).

### 3.2.2 IMS for Small Organic Compounds

***3.2.2.1 Employment of Optimized Experimental Protocols Is an Essential Issue*** In the field of the molecular biology, localization of transcripts is visualized with oligonucleotide probe in situ hybridization, and localization of proteins is visualized using immunohistochemistry based on antibodies. The emergence and continuous development of IMS could add another standard imaging technique for metabolites, whereas we do not have an established visualization technology for them. In fact, until today, the small metabolites (i.e., $m/z < 1000$) have been intensively investigated by IMS and this research application can be further subdivided into two distinct areas: (1) measurement of endogenous small organic compounds and (2) measurement of exogenous compounds (such as administrated drugs). For both, the nature of MS-based detection principle facilitates the IMS as an effective imaging tool for these metabolites in which any chemical labels and probes are not required. Such uniqueness of IMS provides a capability for simultaneous visualization of multiple metabolites, enabling to follow molecular conversion of these small organic compounds (i.e., metabolism itself) between times or conditions (Table 3.2). However, each of such diverse molecular species could have quite different chemical/physical properties, and therefore, in practical, an optimization process of experimental protocol for each analyte is still an essential issue. As a representative example, Figure 3.10 demonstrates that concentration of the organic solvent (in this case, methanol) in the matrix solution affects the detection sensitivity of lipids and peptides. The results showed that a high composition of methanol (80%–100%) was favorable for lipid detection, while a low concentration solution (20%–40%) was favorable for the detection of peptides, indicating that lipids and peptides could be efficiently extracted from tissue sections into organic and nonorganic solvents, respectively.

Figure 3.11 summarizes such key experimental points. As a first point, we have to choose the appropriate ionization method; for the detection of small metabolites, we have alternative choices other than MALDI, such as secondary ion mass spectrometry (SIMS) [15], nanostructure-initiator mass spectrometry (NIMS) [20,21], desorption/ionization on silicon (DIOS) [22], nanoparticle-assisted laser desorptiopn/ionization (nano-PALDI) [23], and even laser desorption/ionization (LDI) [24,25]. We consider that MALDI is still the most versatile method, particularly due to the soft ionization capability of intact analyte. However, other methods each have unique advantages; for example, SIMS and nano-PALDI have achieved higher spatial resolution than conventional MALDI-IMS, and above all, these mentioned alternative methods are all matrix-free methods, and thus can exclude the interruption of the matrix cluster ion. Next, if MALDI is chosen, experimenters should choose a suitable matrix compound, solvent composition, and further matrix application method for their target analyte. All these factors are critical to obtain sufficient sensitivity because they affect efficiency of analyte extraction, condition of cocrystallization, and, above all, analyte–ionization efficiency. In addition, based on the charge state of the analyte molecule, suitable MS polarity (i.e., positive/negative ion detection mode) should be used in MS measurement. Below, we shall describe the key experimental points for MALDI-IMS applications of representative metabolites.

***3.2.2.2 IMS of Endogenous Metabolites: Lipids*** Among the endogenous metabolites, MALDI-IMS for profiling [8,26–28] and visualizing distribution [1,29] of lipids is the best established application area. In the body, numerous lipid species play specific functional roles, for example, energy storage, structural components of cell membranes, and important signaling molecule. Such lipid species may be roughly divided into three large categories: *complex lipids*, which contains phosphate and sugars in their structures (e.g., glycerophospholipids, GPLs); *simple lipids*, which are alcohol fatty acid esters (e.g., acylglycerols); and *derived lipids*, produced via hydrolysis of the simple/complex lipids (e.g., fatty acids). Table 3.3 shows the representative application studies of MALDI-IMS for lipids, and as can be seen, explorations of complex lipids have been the most intensively performed. This may be due to their easily charged structures, for example, phosphate group in phospholipids, sialic acids in gangliosides, and sulfate

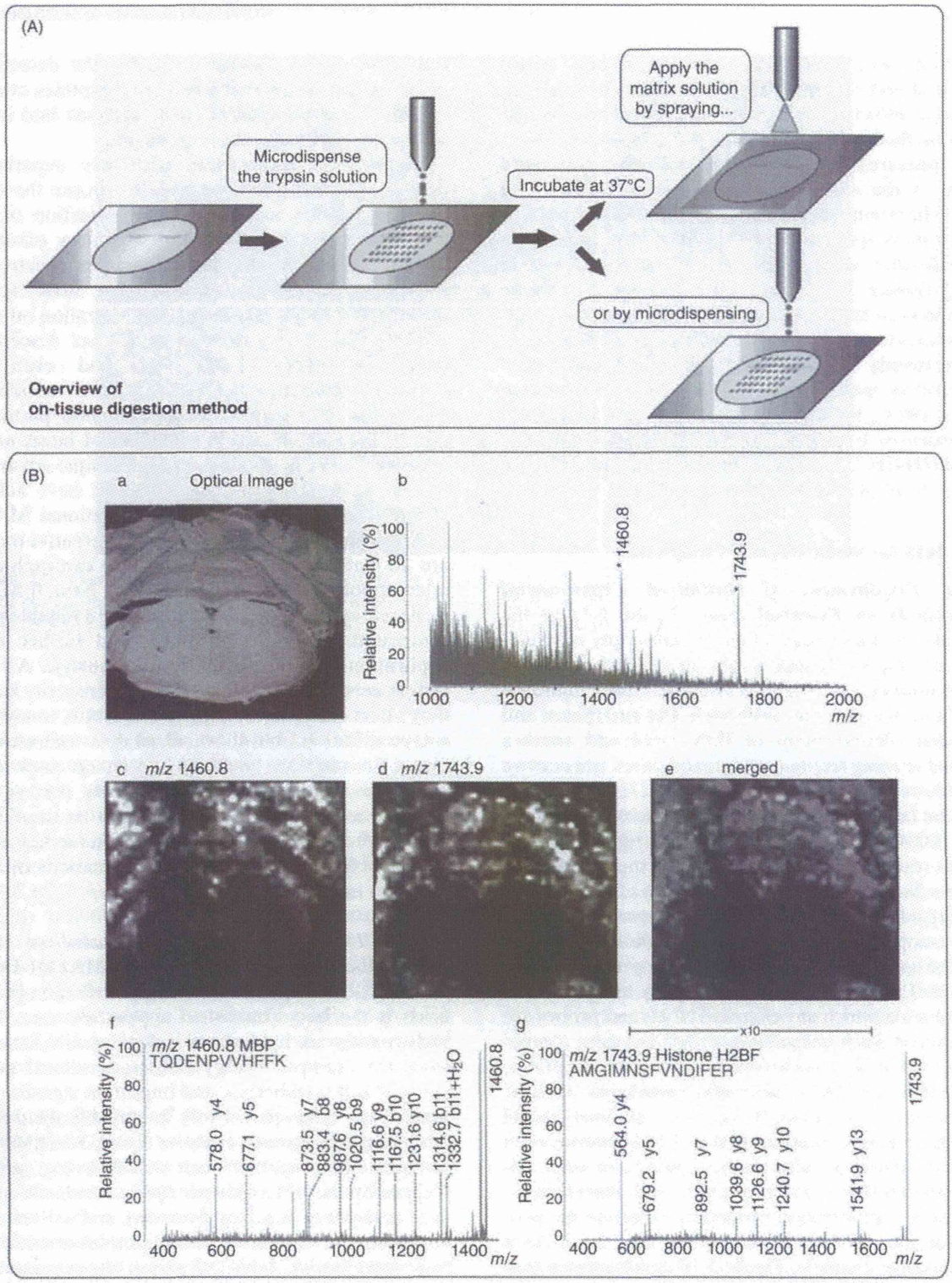


**FIGURE 3.8** Tryptic-digested protein imaging and precursor ion mass spectra with positive ion detection mode. A. A scheme showing overview of on-tissue digestion method. B. An example of IMS of tryptic-digested proteins. (a) Optical image of imaging region and (b) accumulated mass spectrum from imaging region. (c, d) Imaging results of *m/z*1460.8 and 1743.9, which are labeled by asterisks in (b). The merged image (*m/z* 1460.8 and *m/z* 1743.9) is shown in (e). These peaks were identified by direct multistage tandem mass spectrometry (MSn) and were identified as the fragment ions of (f) myelin basic protein (MBP) and (g) histone H2B [18].

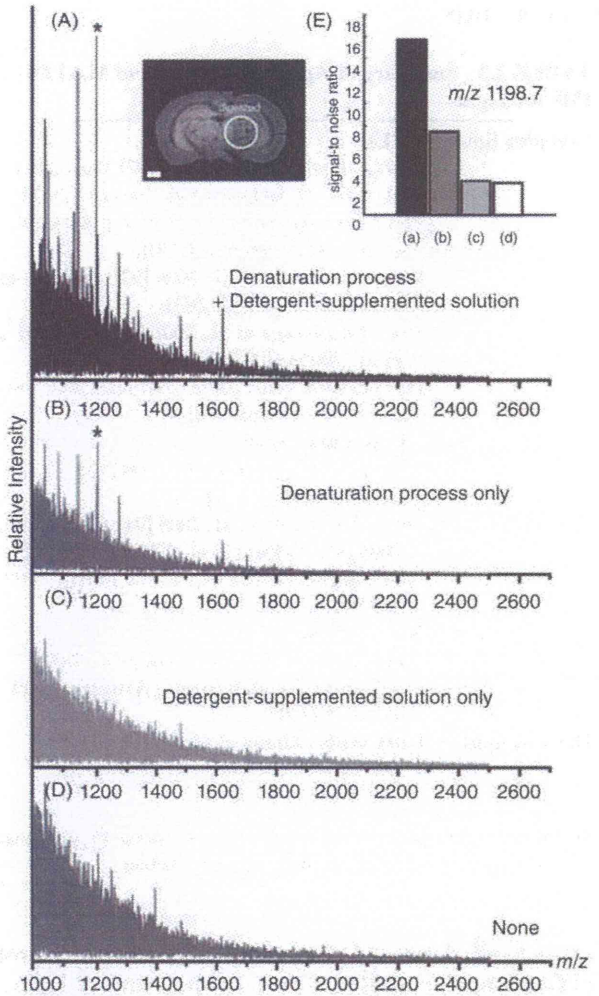


**FIGURE 3.9** On-tissue digestion process was enhanced by the heat-denaturation process and the use of detergent-supplemented trypsin solution. A. Mass spectra obtained from 10-μm mouse cerebellum sections of trypsin-digested position (see inset). B–D. Mass spectrum obtained from the tissue sections prepared with indicated treatment of denaturation and detergent. Asterisks represent the mass peaks at *m/z* 1198.7. E. Signal-to-noise ratio of peak at *m/z* 1198.7 obtained from each tissue section. Bar, 1 μm [19].

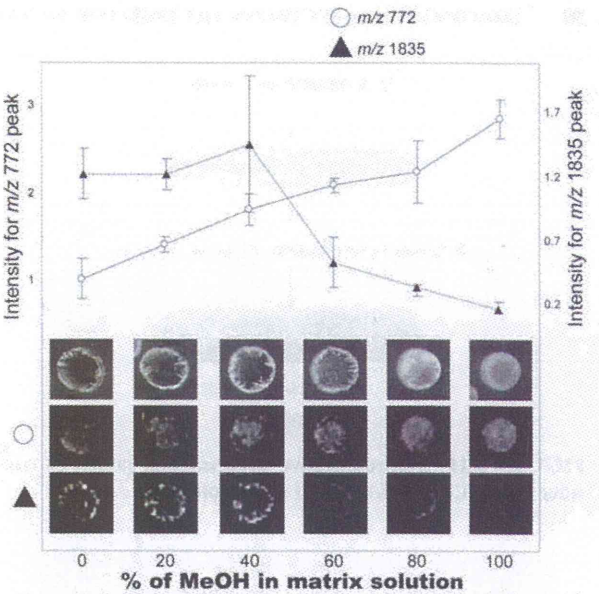


**FIGURE 3.10** Concentration of organic solvent in the matrix solution influences signal detection in the analysis of lipids and peptides. The brain homogenate slices were dispensed with 0.1 μL of DHB solutions containing different concentrations of the organic solvent (0%, 20%, 40%, 60%, 80% and 100% methanol containing 0.1% TFA), and the sensitivity of the signals corresponding to endogenous lipids and peptides was measured. The results showed that a high composition of methanol (80%–100%) was favorable for lipid detection, while a low concentration solution (20%–40%) was favorable for the detection of peptides. The crystal form of the analytes also changed with an increase in the methanol concentration in the matrix solution; needle-like crystals from which peptides were detected changed into aggregates of smaller crystals from which lipids were detected.

**TABLE 3.2 Potential Contribution of IMS for Imaging of Metabolites in Tissues or Cells**

| | Representative Molecular Imaging Method in Tissue or Cells | Probes | Selectivity | Allow Simultaneous Imaging |
|---|---|---|---|---|
| molecular diversity ▲ | | | | |
| DNA | FISH (fluorescence in situ hybridization) | Oligo nucleotide probe | Targeted | + |
| RNA | In situ hybridization | Oligo nucleotide probe | Targeted | + |
| Protein | Immunohistochemistry, green fluorescent protein-fused protein | Antibody | Targeted | + |
| Metabolite (especially lipids) | Imaging mass spectrometry | – | Targeted/ nontargeted | +++ |

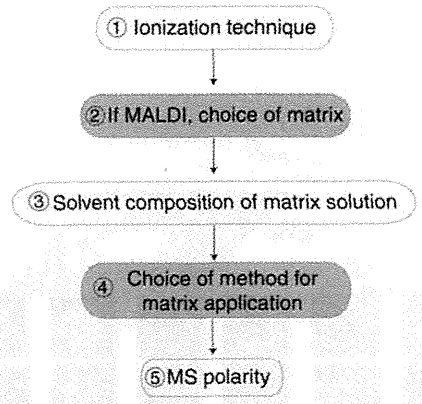


**FIGURE 3.11** Representative experimental points to consider in MALDI-IMS of small metabolites.

group in sulfatides. In particular, GPLs is the most frequent studied topic because their rich amounts in the tissues make the analysis easier [30]. However, for analysis of the noncharged and less-abundant molecular components, development of suitable sample preparation protocol to enhance their sensitivity is necessary. This is especially the case for lipid imaging, in which tissue-washing procedure with organic solvents is omitted because lipids are easily lost or migrate from their original location in tissues. When such a crude sample is subjected to MS analysis, numerous molecular species compete for ionization, and this can gives rise to severe ion suppression effects, degrading the sensitivity of such "difficult" lipids [5–7]. Hence, systematical experimental strategies ranging a wide variety of lipid species must be developed for successful lipid IMS. Figure 3.12 shows a proposed experimental strategy for MALDI-IMS of biological lipids. It is reported that proper choice of MS polarity (positive or negative) and use of suitable matrix solution is critical [31,32].

*Addition of Salt to the Matrix Solution Enhanced the Sensitivity of Lyso-PC (Polar Lipid) Detection But Decreased the Sensitivity of TG (Nonpolar Lipid) Detection* As demonstrated in Figure 3.10, composition of matrix solution is an important and useful "adjustable" parameter to increase the detection sensitivity of target analyte. In addition, if properly used, additive compounds to the matrix solution are another effective factor to achieve selective increase of target analyte signal. In this regard, it is reported that the presence/absence of alkali metal salts in the matrix solution affects the detection sensitivity for polar and nonpolar lipids [32]. Figure 3.13 shows that addition of the potassium acetate to the matrix solution enhanced the sensitivity of lyso-PC (polar lipid) detection, but on the other hand, decreased the sensitivity of triacylglycerol (TG) (nonpolar lipid) detection. The left panel of Figure 3.13 shows that the alkali metal salt in the matrix solution enhanced the sensitivity of phosphatidylcholine (PC) detection, presumably by the merging of $[M+H]^+$ and $[M+K]^+$ ion adduct form into $[M+K]^+$, in the presence of potassium salt additive. Contrastingly, under the presence of a potassium salt, the intensity of TG as the $[M+K]^+$ decreased to approximately half even at 4 mM (right panel). This can be accounted in that the enhancement of ionization for endogenous PCs signals the underexistence of the salt; the signal degradation of neutral lipids was attributed to the ion suppression effect of the enhanced PC ionization.

**TABLE 3.3 Summary of Application Studies of MALDI-IMS for Lipids**

| | |
|---|---|
| Complex lipid | **GPLs**<br>PCs (Astigarraga et al., 2008 [92]; Garrett et al., 2006 [1]; Jackson et al., 2005a,b [26,54]),<br>PEs (Astigarraga et al., 2008 [92]; Jackson et al., 2005a, 2007b [26,58]),<br>PIs (Astigarraga et al., 2008 [92]; Jackson et al., 2005a, 2007b [26,58]),<br>PSs (Astigarraga et al., 2008 [92]; Jackson et al., 2005a, 2007b [26,58]),<br>PGs (Jackson et al., 2005a, 2007b [26,58]), and<br>Cardiolipins (Wang et al., 2007 [31])<br>**Glycosphingolipids**<br>Gandliosides (Chen et al., 2008 [56]; Sugiura et al., 2008 [93]),<br>Sulfatides (Ageta et al., 2008 [94]; Chen et al., 2008 [56]; Jackson et al., 2007b [58]), and<br>Galactocyl-ceramide (Cha and Yeung, 2007 [95]; Taira et al., 2008 [23]) |
| Simple lipid | **Neutral lipids**<br>Triacylglycerols (Astigarraga et al., 2008 [92]) and diacylglycerols (Astigarraga et al., 2008 [101]) |
| Derived lipid | **Fatty acids** (Zhang et al., 2007 [96])<br>**Cholesterol** (Altelaar et al., 2006 [72]; Jackson et al., 2005a [26]) |

PC, phosphatidylcholine; PE, phosphatidylethanolamine; PI, phosphatidylinositol; PS, phosphatidylserine; PG, prostaglandin.

*Generation of Multiple Molecular Ion Adducts from a Single PC Molecular Species Was Suppressed by Adding an Alkali Metal Salt to the Matrix Solution* The addition of alkali metal salts has another advantage: The formation of multiple molecular species with the same nominal mass can be avoided during the analysis of endogenous phospholipids. With the addition of alkali metal salts, the mass spectra of endogenous lipids (in the *m/z* range of 400–900) are simplified to a

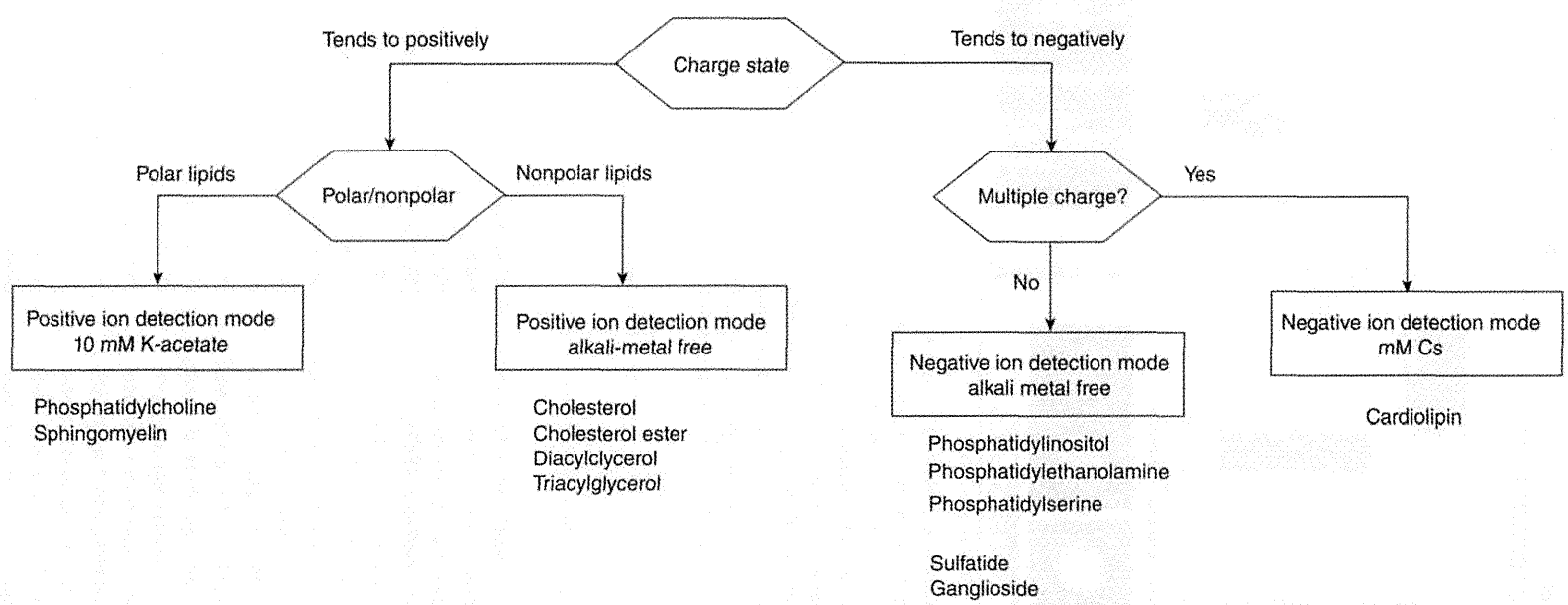


**FIGURE 3.12** Suggested experimental procedure for various lipid molecules.

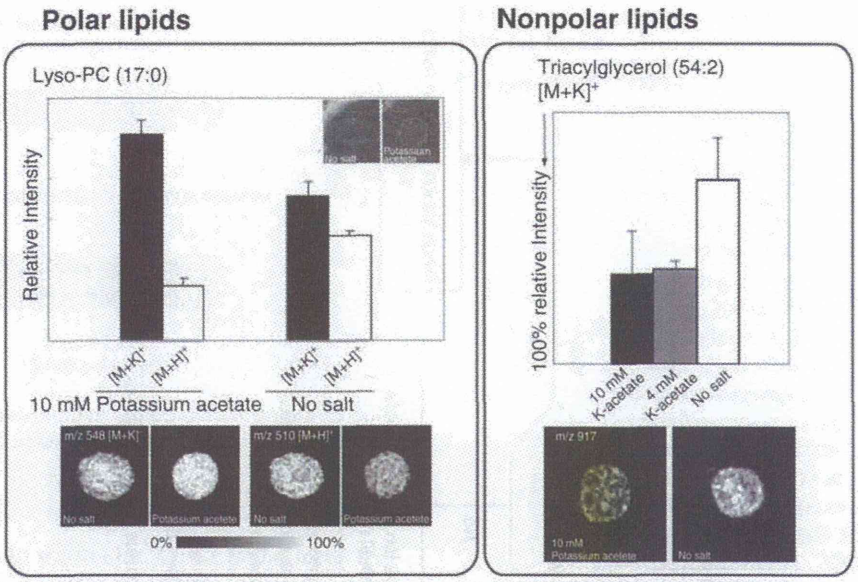


**FIGURE 3.13** Addition of the potassium acetate to the matrix solution enhanced the sensitivity of lyso-PC (polar lipid) detection, but on the other hand, decreased the sensitivity of TG (nonpolar lipid) detection. We dispensed the solution of the reference compounds (0.1 μL) on thin sections of the tissue homogenate. We then sprayed the sections with different matrix solutions and measured the sensitivity of detection of each dispensed compound. We tested polar lipids such as lyso-PC and nonpolar lipids such as cholesterol and TG which tend to be charged positively. The results obtained for PC showed that the alkali metal salt in the matrix solution enhanced the sensitivity of PC detection; the most prominent signal derived from lyso-PC(17:0) was attributed to the $[M+K]^+$ ion when using potassium acetate as the additive, while the generation of the $[M+H]^+$ ion was reduced under the condition. These results can be accounted for the merging of ion adduct form into $[M+K]^+$ in the presence of potassium salt additive. On the other hand, alkali metals salts added to the matrix solution during the detection of nonpolar lipids caused a decrease in the signal sensitivity.

considerable extent since multiple adduct ions formed are merged into a single alkali adduct ion. Figure 3.14 shows the representative mass spectra obtained from the rat kidney sections both in the presence/absence of 10 mM potassium acetate. Since PCs preferentially form cations in the form of alkali metal adducts [26,33,34] and tissues are rich in sodium and potassium salts, peaks due to $[M+H]^+$, $[M+Na]^+$, and $[M+K]^+$ ions are detected in the mass spectra of endogenous PCs (Figure 3.14A). This is a critical problem that needs to be addressed because many molecular species are generated from PCs, and hence, a single peak in the spectrum may correspond to multiple ions. Table 3.4 summarizes the *m/z* values of abundant brain PCs in various ion forms, and it demonstrates that many molecular species share the same nominal mass (as indicated by the same fonts or styles). For example, the mass of a protonated PC(diacyl-16:0/20:4) molecule is identical to that of a sodiated PC(diacyl-16:0/18:1) ion (*m/z* 782), as can be seen in Figure 3.14A. In fact, MS/MS analysis of the peak appearing at *m/z* 782 in the absence of the potassium salt shows that this peak actually corresponds to three different PC ions: $[PC(diacyl\text{-}16:0/20:4)+H]^+$, $[PC(diacyl\text{-}16:0/18:1)+Na]^+$, and $[PC(1\text{-}alkyl\text{-}16:0/18:2)+K]^+$. This can be confirmed from the MS/MS spectra shown in Figure 3.14B(e–f); the peak at *m/z* 782 corresponds to three type of PCs which are a protonated PC ion (by a diagnostic peak at *m/z* 184 [a]), a sodiated PC ion (by *m/z* 147 [b]), and a potassiated PC ion (by *m/z* 163 [c]). On the other hand, upon addition of the potassium salt, peaks due to the aforementioned forms of the PC ions were separated into two distinct peaks at *m/z* 798 and 820, corresponding to $[PC(diacyl\text{-}16:0/18:1)+K]^+$ and $[PC(diacyl\text{-}16:0/20:4)+K]^+$, respectively (Figure 3.14A). In addition, MS/MS analysis of the spectra clearly shows that only potassiated PC molecules are present in the mass peaks (Figure 3.14B[g–h]). As can be seen from Table 3.4, by merging into $[M+K]^+$ ion, most of such mass sharing of abundant PC species can be avoided except that of isobaric species.

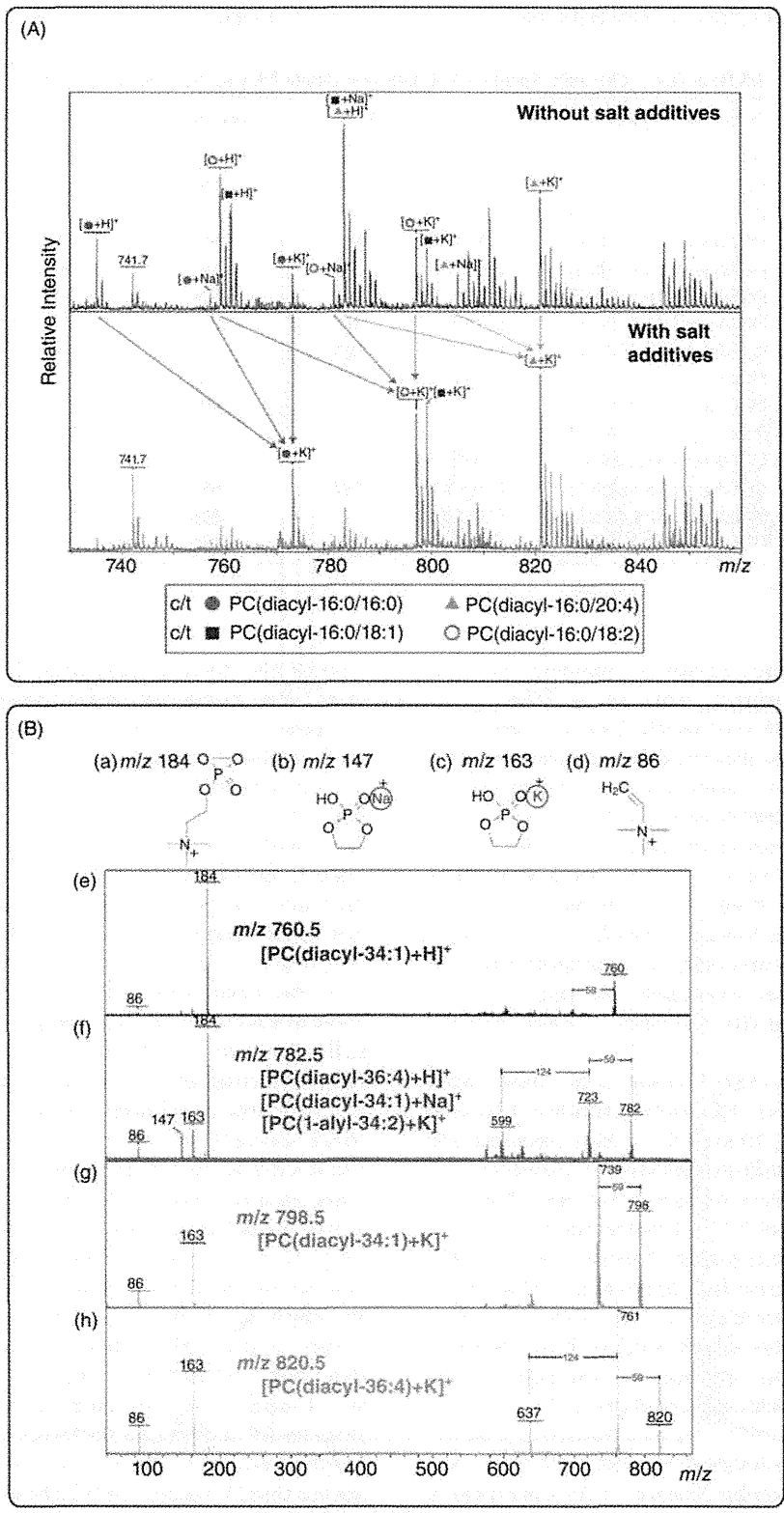


**FIGURE 3.14** Generation of multiple molecular ion adducts from a single PC molecular species was suppressed by adding an alkali metal salt to the matrix solution. A. Generation of multiple molecular ions from a single PC molecule was suppressed by adding an alkali metal salt to the matrix solution. Spectra obtained from sections of rat brain homogenate in the presence/absence of potassium acetate in the matrix solution are shown. With the addition of potassium acetate to the matrix solution, multiple molecular ion forms of PCs merged into a single potassiated PC ion. B. Structure of the diagnostic ions for (a) protonated PC at *m/z* 184; (b) sodiated PC at *m/z* 147; (c) potassiated PC at *m/z* 163. MS/MS spectra of ion peaks at (e) *m/z* 760 and (f) 782 in the absence of potassium acetate and spectra of ions peaks at (g) *m/z* 798 and (h) 820 in the presence of potassium acetate are also shown. c/t, corresponding to.

**TABLE 3.4 The *m/z* Values of Abundant Brain PCs as Various Ion Forms**

| Molecular Species | PC | $[M+H]^+$ | $[M+Na]^+$ | $[M+K]^+$ |
|---|---|---|---|---|
| PC(diacyl 16:0–18:1) | C34:1 | 760 | 782 | 798 |
| PC(diacyl 16:0–16:0) | C32:0 | 734 | 756 | 772 |
| PC(diacyl 18:0–18:1) | C36:1 | 788 | *810* | 826 |
| PC(diacyl 16:0–20:4) | C36:4 | 782 | 804 | 820 |
| PC(diacyl 16:0–18:0) | C34:0 | 762 | 784 | 800 |
| PC(diacyl 16:0–22:6) | C38:6 | **806** | 828 | 844 |
| PC(diacyl 18:0–20:4) | C38:4 | *810* | ***832*** | 848 |
| PC(diacyl 18:1–20:4) | C38:5 | **808** | 830 | 846 |
| PC(diacyl 18:0–22:6) | C40:6 | 834 | 856 | 872 |
| PC(diacyl 18:1–18:1) | C36:2 | 786 | **808** | 824 |
| PC(diacyl 16:0–16:1) | C32:1 | 732 | 754 | 770 |
| PC(diacyl 18:1–22:6) | C40:7 | ***832*** | 854 | 870 |
| PC(diacyl 16:0–20:3) | C36:3 | ***784*** | **806** | 822 |
| PC(diacyl 18:0–18:2) | C36:2 | 786 | **808** | 824 |
| PC(diacyl 18:1–18:2) | C36:3 | ***784*** | **806** | 822 |

*For Negatively Charged Lipids Containing Multiple Negative Charted Structures, Addition of Alkali Metal Salt Enhanced Generation of Singly Charged Molecular Ions* Alkali-metal salts dissolved in the matrix solution enhanced generation of singly charged ion molecules which contain the multiple negatively charged structures; during ionization, residual charged groups in their structures were neutralized by adduct formation with alkali metal cations, and as a result, singly charged ions could be efficiently generated. Since in MALDI process, much less multiple charged ions could be generated than that of ESI, the salt addition eventually can improve their sensitivity by promoting the efficiency of single-charged ion generation.

In the study of Hay-Yan J. Wang et al., they added 100 mM of cesium iodide to a matrix solution (docosahexaenoic acid [DHA] 30 mg/mL in 50% ethanol) and successfully profiled multiple species of cardiolipin as single-charged molecular ions by neutralizing additional phosphate group (Figure 3.15). This treatment also benefits to integrate the ion adduct form to $[M+Cs-2H]^-$ [31]. That may be the case for gangliosides, which have multiple sialic acids in their sugar chain. Taken together, for the analysis of lipids which tend to have multiple charges, the addition of appropriate concentration of alkali metal salt is advantageous (Figure 3.12).

*MALDI-IMS of Phospholipids Revealed Cell-Selective Production of PC Molecular Species* GPLs comprise a large molecular family in which phosphoric acid is esterified to a glycerolipid. They are subdivided into distinct classes (e.g., PCs, phosphatidylethanolamines, and phosphatidylinositols) based on the structure of the head group linked to the phosphate, attached at the *sn-3* position of the glycerol backbone. They are further subdivided into numerous molecular species on the basis of the composition of the fatty acids linked to the *sn-1* and *sn-2* positions of the glycerol backbone [30]. Using IMS, we can image not only these multiple classes but also related molecular species simultaneously. In particular, the capability to determine the distinct localization of each molecular species, that is, to elucidate the distinct fatty acid composition of biological membranes in different tissue locations, is an important advantage of IMS [30] (Figure 3.16).

In the brain, among the classes of GPLs, PCs are the most abundant structural component of neural and glial cell membranes, and the fatty acid constituents of PCs (i.e., molecular species) influence the membrane's physical properties, including fluidity and curvature [35–38]. Since several types of fatty acids, especially polyunsaturated fatty acids (PUFA), in the PCs are released and converted in response to extracellular stimuli into bioactive lipids that mediate important biological processes [39], information on the distinct distributions of PUFA-containing molecular species is quite valuable [40,41]. By applying high-magnification IMS to the cerebella cortex, a docosahexaenoic acid-containing phosphatidylcholine (DHA-PC), namely PC(diacyl-18:0/22:6), was found to be enriched in the Purkinje cell layer (Figure 3.17). Optical observation of successive hematoxylin and eosin (HE)-stained brain sections also suggested that PC(diacyl-18:0/22:6) was selectively detected in Purkinje cells (Figure 3.17, arrowheads) and in molecular layers (MLs) in which dendrites of Purkinje cells exist. In contrast, granule cells were impoverished in another DHA-PC, namely PC(diacyl-18:0/22:6). Interestingly, a complementary distribution of two other